JOURNAL OF SPACECRAFT AND ROCKETS
Vol. 45, No. 5, September–October 2008

Engineering Note

ENGINEERING NOTES are short manuscripts describing new developments or important results of a preliminary nature. These Notes should not exceed 2500 words (where a figure or table counts as 200 words). Following informal review by the Editors, they may be published within a few months of the date of receipt. Style requirements are the same as for regular contributions (see inside back cover).

Damping Behavior of Sloshing Liquid in Laterally Excited Cylindrical Propellant Vessels

Tim Arndt* and Michael Dreyer†
University of Bremen, 28359 Bremen, Germany

DOI: 10.2514/1.35019

I. Introduction

LIQUID sloshing still appears as an undesired phenomenon concerning most applications for fluid management in space transportation vehicles. Necessary to boost the vehicle from Earth's surface to the orbital position, rocket propellant represents the most significant weight fraction influencing the launcher's attitude control. In this connection, one field of interest is the understanding of the propellant damping properties in rocket tanks.

Previously, fundamental theoretical work was accomplished by Lamb [1] and Miles [2] generating the basic equations based on the potential theory. Later, Abramson [3] experimentally investigated the dynamic behavior in moving containers for NASA. Recently, this work was rewritten by Dodge [4], in which numerical methods were updated using more efficient simulation codes. Also Bauer [5–7] and Bauer and Eidel [8] provided major contributions to enhance the understanding on this field.

Investigations of damping characteristics, however, became of major interest during the 1960s, when American and Russian space programs were strongly supported by their own governments, focusing on the manned exploration of Earth's orbit and the moon. Premises for these missions are launcher systems requiring more powerful engines and larger propellant tanks. Basic experimental work studying the damping behavior of sloshing liquid was done by Mikishev and Dorozhkin [9] and Stephens et al. [10] considering cylindrical tank shapes. Other geometries such as spherical and lenslike shapes were explored by Abramson [3] and later confirmed by Dodge [4] and Ibrahim [11]. Nonlinear effects are observed in cylindrical tanks, while excited at close to the first natural frequency, in which the liquid surface forms large-amplitude breaking waves. This phenomenon also occurs in sector-compartmented cylindrical vessels, in which nonlinear effects are even stronger [3,5].

In this work, we perform experiments with cylindrical tank geometries, including the most prevalent flat-, concave-, and convex-bottom shapes. Experimental damping results are correlated to numerical simulations using the commercial computational fluid dynamics (CFD) software Flow3D. Particularly, close to the first natural frequency, our experimental results are applied to predict the amplitude response behavior of sloshing-liquid systems.

Presented as Paper 5162 at the 43rd AIAA/ASME/SAE/ASEE Joint Propulsion Conference and Exhibit, Cincinnati, OH, 8–11 July 2007; received 7 October 2007; revision received 12 February 2008; accepted for publication 24 February 2008.

*Engineer, Fluid Dynamics, Mechanical Engineering, Center of Applied Space Technology and Microgravity; arndt@zarm.uni-bremen.de. Member AIAA.

†Engineer, Project Management, Fluid Dynamics, Center of Applied Space Technology and Microgravity; dreyer@zarm.uni-bremen.de.

II. Experimental Setup

As illustrated in Fig. 1, the sloshing platform (1) is driven by the electric engine (2). By means of the crank drive (3), the rotational motion is transformed into sinusoidal oscillations. Hereby, the oscillations are defined by the excitation amplitude y_A and the excitation frequency $f = \omega/2\pi$, where ω is the angular velocity of the drive shaft. To enable the one-degree-of-freedom excitation, the sloshing platform is installed on three grooved ball bearings. On top, the sloshing platform is equipped with the modular test vessel (4). Three cylindrical vessel configurations are available for the tests, including the well-known flat-bottom geometry [3,4,7,9,10] illustrated in Fig. 1a, the concave-bottom geometry [3,4,9] illustrated in Fig. 1b, and the convex-bottom geometry illustrated in Fig. 1c. The radius of the cylindrical vessel part in all cases is $R = 145$ mm. The fill level is defined as H, for which the deepest position in the test vessel that is filled with liquid is the origin of the coordinate system (x, y, z). All test vessel parts are made from acrylic glass to enable optical access during the experimental run.

The test facility allows excitation frequencies up to $f = 3.0$ Hz, whereas the excitation amplitude is limited to $y_A = 2.87$ mm. For data acquisition, the test facility is equipped with a high-speed-camera system. This enables the measurement of the wave amplitude z_w given by the liquid-surface contour on the tank wall. Measurement errors determining z_w are estimated up to 7%. Deionized water at approximately 20°C is used as the test liquid; the density is $\rho = 998.20$ kg/m^3, and the kinematic viscosity is $\nu = 1.004 \times 10^{-6}$ m^2/s.

Dimensionless numbers are a convenient method to scale actual quantities into laboratory size. Considering a laterally excited test vessel, the viscous damping can be characterized by the Galilei number, defined as the ratio of the gravitational forces to the viscous forces, yielding

$$\mathbf{Ga} = \frac{gR^3}{\nu^2} \tag{1}$$

where g is the gravitational acceleration. The influence of surface tension σ (particularly, under zero gravity) is described by the Bond number

$$\mathbf{Bo} = \frac{\rho g R^2}{\sigma} \tag{2}$$

Table 1 gives an overview of the actual scaling between the experiment and the full-size tanks under real conditions.

III. Numerical Methods

Numerical simulations are performed using the commercial CFD solver FLOW-3D Ver. 9.1.1. (Flow Science. Inc.) that is based on the volume-of-fluid technique. The test vessel is resolved by a cubic mesh with a total cell amount of 72,900 cells. Excitations are implemented based on the acceleration in the sloshing direction:

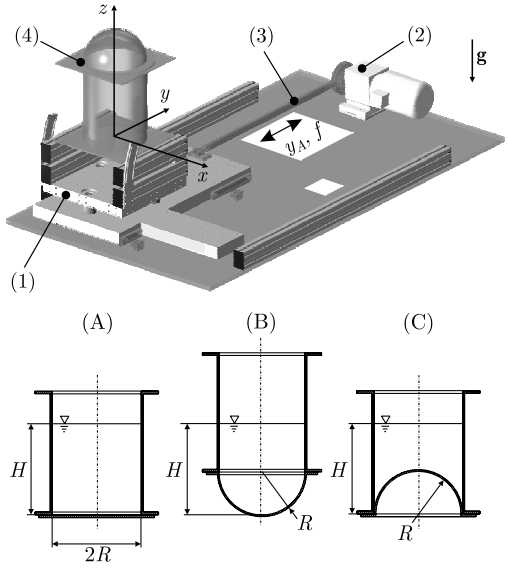

Fig. 1 Illustration of the sloshing test facility at the Center of Applied Space Technology and Microgravity, including sketches of the test vessels; base plate dimensions are 2.2 × 1.2 m.

$$a_y(t) = y_A[-\omega^2 \cos(\omega t) + \lambda\omega^2 \cos(2\omega t)] \tag{3}$$

where $\lambda = y_A/l$ is the drive ratio and $l = 1100$ mm is the cone rod length. Because $\lambda \ll 1$, the oscillation described by Eq. (3) is approximately harmonic. Assuming a passive gas phase, the one-fluid free-surface method is applied to solve the momentum and the continuity equation, and the momentum advection is set to the first order. Excited simulation cycles are performed until reaching the steady state after 180 s. The restart point of the calculation is synchronized with our displacement sensor data to define the exact point of the engine stop. Then the calculation is repeated without excitation so that the sloshing liquid can decay.

IV. Damping

Damping experiments are performed for certain fill ratios between $0.2 \le H/R \le 2$ after exciting the liquid corresponding to 90% of the respective first natural frequency:

$$f_{11}^2 = \frac{\varepsilon_{11} g}{4\pi^2 R} \tanh\left[\varepsilon_{11} \frac{H}{R}\right] \tag{4}$$

where $\varepsilon = 1.84$ is given by the first root of the derivative of the Bessel function of the first kind. However, reaching the steady state after approximately 3 min, the excitation is abruptly stopped so that the sloshing liquid can decay exponentially. The damping behavior of sloshing systems is quantified by means of the dimensionless damping ratio $\gamma = \Lambda/\Delta$, a measure that is frequently found in the literature [3,10,11]. In this connection,

$$\Lambda = \frac{\ln z_{w,1} - \ln z_{w,i}}{i} \tag{5}$$

is the logarithmic decrement based on the wave decay. The denominator is the deepwater damping parameter [4,11] $\Delta \propto \mathbf{Ga}^{-1/4}$, valid for $H/R > 1$.

The dependency of γ on the fill level is shown in Fig. 2. For flat-bottom configurations, the development of the damping is described by an analytical approach found by Stephens et al. [10]. They confined the influence of viscosity to a thin boundary layer at the vessel wall, in which frictional interactions between the liquid and the vessel wall dominate the liquid motion. This approach yields [10,11]

$$\Lambda = K\mathbf{Ga}^{-1/4}\left[\frac{1 + 2[1 + 2(1 - H/R)]}{\sinh(2\varepsilon_{11}H/R)\tanh^{1/4}(\varepsilon_{11}H/R)}\right] \tag{6}$$

where K is an experimental parameter [10]. As shown in Fig. 2a, our experimental data fit the theoretical prediction reasonably well, with the exception of $H/R < 0.5$. This is not surprising, because the measurement error for small fill levels is much higher.

Damping results of the concave-bottom experiments are plotted in Fig. 2b. Particularly, for $H/R < 1$, we observed higher damping ratios, caused by the spherical-bottom geometry. Again, the damping

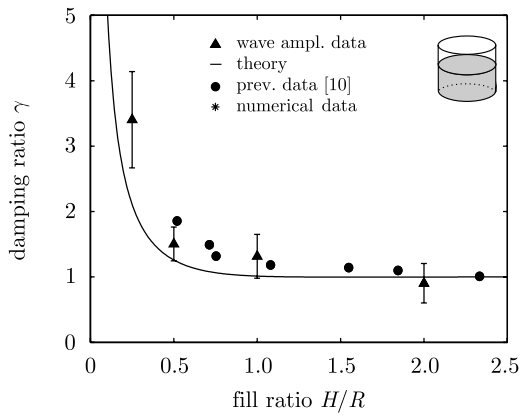

a) Flat-bottom geometry

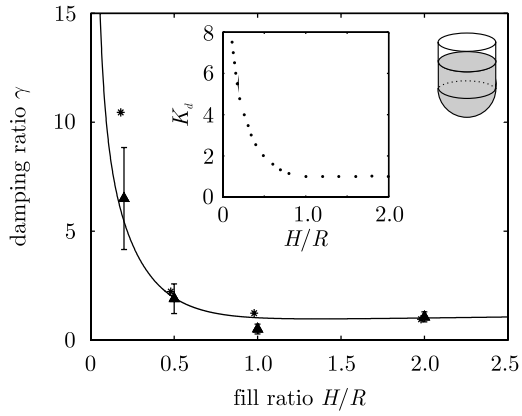

b) Concave-bottom geometry

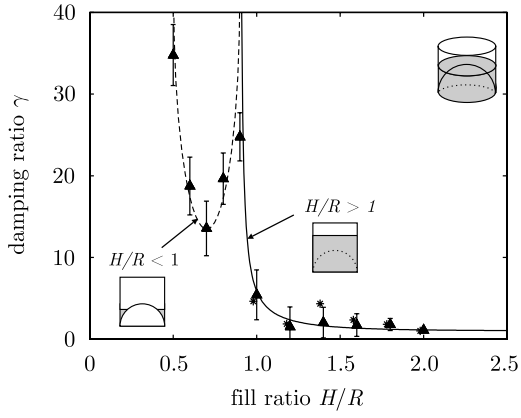

c) Convex-bottom geometry

Fig. 2 Damping ratio as a function of the fill ratio for each bottom geometry.

Table 1 Scaling of experimental parameters

Fluid	g, m/s^2	**Ga**	**Bo**
Water	9.81×10^0	2.97×10^{10}	2.82×10^3
Liquid hydrogen	9.81×10^0	4.20×10^{15}	2.17×10^6
Liquid hydrogen	9.81×10^{-2}	4.20×10^{13}	2.17×10^4
Liquid oxygen	9.81×10^0	5.24×10^{15}	5.38×10^6
Liquid oxygen	9.81×10^{-2}	5.24×10^{13}	5.38×10^4

can be expressed by a theoretical relation that is similar to the analytical approach in Eq. (6). For concave bottoms, the damping relation is supplemented by the geometry factor K_d determined by Mikishev and Dorozhkin [9]. The development of K_d is plotted in the inset of Fig. 2b. However, for the concave bottom considered here, $K = 10.32$ is found to be two times greater than observed for the flat-bottom experiment, where $K = 5.23$.

As shown in Fig. 2c, γ for the convex-bottom geometry behaves differently from the flat- and concave-bottom results. The development of the experimental data allows the assumption to divide the vessel in two regions. On one side, the results show toroidal characteristics [3,4] for $H/R < 1$, as indicated by the dashed line in Fig. 2c, where the convex dome appears in the middle of the test vessel. On the other side, the damping for $H/R > 1$ matches a regular cylindrical flat-bottom tank, indicated by the solid line in Fig. 2c. Again, the experimental parameter yields $K = 5.32$. Numerical simulations are performed for $H/R \geq 1$. In spite of the complex vessel geometry, the calculated γ fits the experimental data reasonably well.

V. Response Curves

According to Scanlan and Rosenbaum [12] and, more recently, Dodge [4] and Ibrahim [11], a laterally excited liquid with a free surface can be considered as a pendulum or a spring mass system. In the latter case, the liquid motion can be described by an ordinary differential equation, such as

$$\ddot{y}(t) + 2D\omega_{11}\dot{y}(t) + \omega_{11}^2 y(t) = y_A \omega_{11}^2 \cos(\omega t) \tag{7}$$

With respect to the linear theory of damped oscillations, the damping factor D can be expressed in terms of the logarithmic decrement, so that

$$D = \Lambda[4\pi^2 + \Lambda^2]^{-1/2} \tag{8}$$

Because we only consider motions after reaching the steady state, the particular solution of Eq. (7) is

$$y(t) = y_A B \cos(\omega t - \phi) \tag{9}$$

and the homogeneous solution can be neglected. Here, ϕ describes the phase shift. The amplitude ratio $B = z_w/y_A$ is a dimensionless measure of the wave amplitude, yielding

$$B = C[(1 - \eta^2)^2 + 4D^2\eta^2]^{-1/2} \tag{10}$$

where $C \approx 1$ is a correction factor to fit our data, and $\eta = \omega/\omega_{11}$ is the dimensionless frequency ratio. Close to the first natural frequency, where $0.9 \leq \eta \leq 1.1$, a vertical baffle is used to prevent any rotational liquid motion. A nonlinear approach is applied to express the occurring effects. In this case, the spring representing the liquid reset force does not satisfy Hooke's law. The spring term $\omega_{11}^2 y(t)$ in Eq. (7) is supplemented by the cubic expression $\omega_{11}^2 \alpha y^3(t)$ to integrate the nonlinear behavior. In this term, the degree of nonlinearity is expressed by the deflection coefficient $\alpha = \mathcal{O}(10^{-5})$. Considering the dimensionless time scale $\tau = \omega_{11} t$ and substituting

$$y'(\tau) = \frac{\dot{y}(t)}{\omega_{11}} \tag{11}$$

as well as

$$y''(\tau) = \frac{\ddot{y}(t)}{\omega_{11}^2} \tag{12}$$

into Eq. (7), leads to the Duffing equation:

$$y''(\tau) + 2Dy'(\tau) + y(\tau) + \alpha y^3(\tau) = y_A \cos(\eta\tau) \tag{13}$$

By applying the method of harmonic balance, the nonlinear term αy^3 is transferred into the linear approximation $\alpha\beta y$. Because the oscillations are assumed to be harmonic, the linearization factor corresponds to $\beta = 3\alpha z_w^2/4$. Then Eq. (13) can be rewritten

$$y''(\tau) + 2Dy'(\tau) + \eta_B^2 y(\tau) = y_A \cos(\eta\tau) \tag{14}$$

where $\eta_B^2 = 1 + \beta$. Equation (9) is solved analogous to the ordinary differential equation in Eq. (10), leading to a particular solution

$$y(\tau) = y_A B \cos(\eta\tau - \phi) \tag{15}$$

The amplitude ratio yields

$$B = C\left[\left(\eta_B^2 - \eta^2\right)^2 + 4D^2\eta^2\right]^{-1/2} \tag{16}$$

Results for the flat-bottom geometry are provided in Fig. 3a, in which response curves for different fill ratios are plotted for each vessel configuration. The influence of damping is identified by the size of the response peak, because the smaller peak corresponds to the more

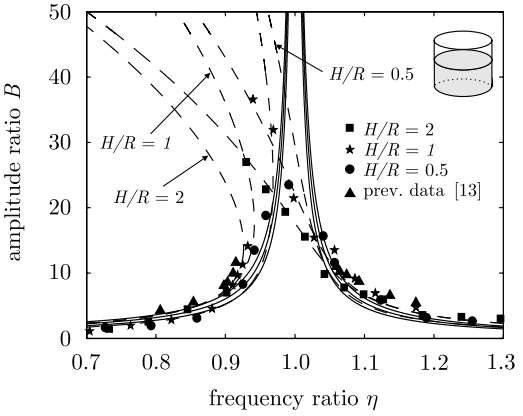

a) Flat-bottom geometry

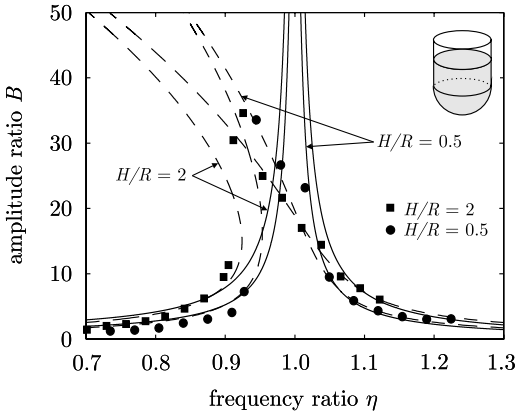

b) Concave-bottom geometry

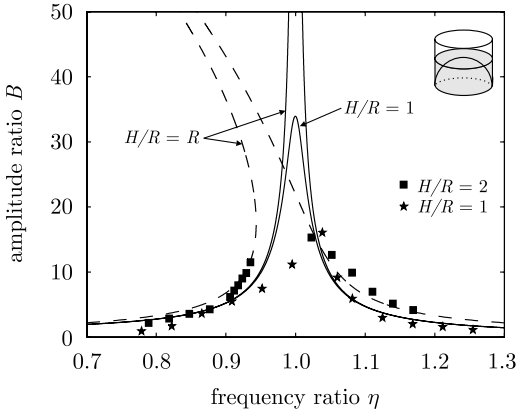

c) Convex-bottom geometry

Fig. 3 Response curves as functions of the frequency for each bottom geometry; solid curves are based on the linear theory in Eq. (10), and dashed lines correspond to the nonlinear theory in Eq. (16).

damped system. While considering the amplitude close to the first natural frequency, in which a baffle is used to prevent liquid swirling, it came out that our linear theory is only applicable for $\eta < 0.9$ and $\eta > 0.9$. In fact, the response characteristics close to f_{11} can be associated with our nonlinear model introduced in Eq. (16). However, plotting Eq. (16) yields the typical nonlinear development, in which the characteristic resonance peak is shifted to the left side. In this connection, the deflection coefficient α is approximately four times smaller for $H/R = 0.5$ than it appears for $H/R = 2$.

Similar characteristics are observed for the concave-bottom vessel, as shown in Fig. 3b. Again, a vertical baffle is used close to f_{11} to prevent liquid swirling. For $H/R = 2$, for which the influence of the bottom can be neglected, the nonlinear response behavior matches the corresponding result achieved with the flat bottom. However, a different behavior is observed for $H/R = 0.5$; the nonlinear behavior seems more obvious for the concave-bottom geometry than it appears in the flat-bottom vessel. The deflection coefficient α is approximately two times smaller than when it emerges for $H/R = 2$.

Results for the convex-bottom vessel are provided in Fig. 3c. For $H/R = 2$, the response curve shows similar properties, as observed during the flat-bottom experiment for $H/R = 1$. This behavior supports our assumption that convex-bottom vessels can be divided into two parts, whereas the convex part may be neglected for fill ratios $H/R \geq 2$. For $H/R = 1$, for which the liquid surface touches the top of the convex dome, the damping is five times higher than it appears for other geometries. Our data here differ from the predicted curve. An explanation can be given by the fact that our data acquisition here is extremely difficult to implement, because occurring wave amplitudes are very small and noisy.

VI. Conclusions

The decay experiments provide insight into the damping behavior of sloshing liquid, considering flat-, concave-, and convex-bottom geometries. As shown in Figs. 2a and 2b, the damping significantly increases for $H/R \leq 1$ and remains on the level of the deepwater damping for $H/R > 1$. Experiments using the convex-bottom geometry suggest a different impression. The test vessels can be divided into two parts, and the boundary between them is located at $H/R \approx 1$. For $H/R < 1$, the damping is similar to the γ observed in toroidal tanks [3,4]. This is different for fill ratios $H/R > 1$, for which the damping appears proportional to the γ observed in flat-bottom vessels.

To get a better understanding of the response behavior in laterally excited propellant tanks, the sloshing characteristics are specified by an ordinary differential equation describing a spring mass system. For frequency ratios $\eta < 0.9$ and $\eta > 1.1$, the linear model prediction in Eq. (10) is experimentally confirmed by our wave-amplitude data, as shown in Fig. 3. This behavior is different close to the first natural frequency, when $0.9 \leq \eta \leq 1.1$. The liquid response satisfies our nonlinear model that is summarized in Eq. (16). According to our observations, the nonlinear phenomenon can be traced back to the vertical baffle applied to prevent liquid swirling. At the liquid surface, the baffle splits the vessel into two parts, leading to a sector tank consisting of two identical semicircular areas. This confirms previous studies [3,5] in which nonlinear effects in cylindrical compartment tanks were observed.

A few questions arise from this work, particularly, considering our nonlinear model introduced in Eq. (16). Based on our experimental results, the deflection coefficient α is basically dependent on the fill level and is only related to the vessel geometry to a small extent. Because the observed behavior is attributed to the nonlinear spring component $\omega_{11}^2 \alpha y^3(t)$, it is not clear how α is functionally connected to the fill level. This represents an area that will need further investigation.

Acknowledgments

The funding of the research project by the German Federal Ministry of Education and Research (BMBF) through the DLR, German Aerospace Center under grant 50RJ0011 is gratefully acknowledged. Furthermore, the authors acknowledge the support of their project partner Astrium GmbH Space Transportation in providing the sloshing facility.

References

[1] Lamb, H., *Hydrodynamics*, 7th ed., Cambridge Univ. Press, Cambridge, England, U.K., 1945.

[2] Miles, J. W., "On the Sloshing of Liquid in a Cylindrical Tank," Ramo-Woolridge Corp., Guided Missile Research Div., Rept. GM-TR-18, Apr. 1956.

[3] Abramson, H. N., "The Dynamic Behavior of Liquids in Moving Containers," NASA SP-106, 1966.

[4] Dodge, F. T., *The New Dynamic Behavior of Liquids in Moving Containers*, Southwest Research Inst., San Antonio, TX, 2000.

[5] Bauer, H. F., "Fluid Oscillations in the Containers of a Space Vehicle and Their Influence on Stability," NASA TRR-187, 1964.

[6] Bauer, H. F., "Hydroelastische Schwingungen im Aufrechten Kreiszylinder," *Zeitschrift für Flugwissenschaften*, Vol. 18, No. 4, Apr. 1970, pp. 117–134.

[7] Bauer, H. F., "On the Destabilizing Effect of Liquids in Various Vehicles (Part 1)," *Vehicle System Dynamics*, Vol. 1, No. 3, Dec. 1972, pp. 227–260.
doi:10.1080/00423117208968429

[8] Bauer, H. F., and Eidel, W., "Oscillations of a Viscous Liquid in a Cylindrical Container," *Aerospace Science and Technology*, Vol. 1, No. 8, Dec. 1997, pp. 519–532.
doi:10.1016/S1270-9638(97)90001-8

[9] Mikishev, G. N., and Dorozhkin, N. Y., "Experimental Investigation of Free Oscillations of a Liquid in Tanks," *Izvestiya Akademii Nauk SSSR, Otdelenie Mehanika i Mashinostroenie*, Vol. 4, 1961, pp. 48–83 (in Russian).

[10] Stephens, D. G., Leonard, H. W., and Perry, T. W., "Investigations of the Damping of Liquids in Right-Circular Cylindrical Tanks, Including the Effects of a Time-Variant Liquid Depth," NASA Langley Research Center, GCA-TR-61-12-N, Hampton, VA, 1962.

[11] Ibrahim, R. A., *Liquid Sloshing Dynamics*, Cambridge Univ. Press, Cambridge, England, U.K., 2005.

[12] Scanlan, R. H., and Rosenbaum, R., *Introduction to the Study of Aircraft Vibration and Flutter*, Macmillan, New York, 1951.

[13] Royon-Lebeaud, A., Hopfinger, E. J., and Cartellier, A., "Liquid Sloshing and Wave Breaking in Circular and Square-Base Cylindrical Containers," *Journal of Fluid Mechanics*, Vol. 577, 2007, pp. 467–494.
doi:10.1017/S0022112007004764

L. Peterson
Associate Editor